RECOMMENDATION ITU-R F.1096

METHODS OF CALCULATING LINE-OF-SIGHT INTERFERENCE INTO RADIO-RELAY SYSTEMS TO ACCOUNT FOR TERRAIN SCATTERING*

(Question ITU-R 129/9)

(1994)

The ITU Radiocommunication Assembly,

considering

a) that interference from other radio-relay systems and other services can affect the performance of a line-of-sight radio-relay system;

b) that the signal power from the transmitting antenna in one system may propagate as interference to the receiving antenna of another system by a line-of-sight great-circle path;

c) that the signal power from the transmitting antenna in one system may propagate as interference to the receiving antenna of another system by the mechanism of scattering from natural or man-made features on the surface of the Earth;

d) that terrain regions that produce the coupling of this interference may not be close to the great-circle path, but must be visible to both the interfering transmit antenna and the receive antenna of the interfered system;

e) that the component of interference power that results from terrain scattering can significantly exceed the interference power that arrives by the great-circle path between the antennas;

f) that efficient techniques have been developed for calculating the power of the interference scattered from terrain,

recommends

1. that the effects of terrain scatter, when relevant, should be included in calculations of interference power when the interference is due to signals from the transmitting antenna of one system into the receiving antenna of another and when either or both of the following conditions apply (see Note 1):

1.1 there is a line-of-sight propagation path between the transmitting antenna of the interfering system and the receiving antenna of the interfered system;

1.2 there are natural, or man-made, features on the surface of the Earth that are visible from both the interfering transmit antenna and the interfered receive antenna;

2. that the methods given in Annex 1 be used to calculate the contribution of interference due to terrain scatter.

Note 1 – Specular reflections or propagation by diffraction are not treated by the calculation methods described in this Recommendation.

---

* Recommendation ITU-R PN.452 (Prediction procedure for the evaluation of microwave interference between stations on the surface of the Earth at frequencies above about 0.7 GHz) in Radiocommunication Study Group 3 (former Study Group 5) addresses other propagation mechanisms. This Recommendation should be brought to the attention of Radiocommunication Study Group 3.

ANNEX 1

Interference to radio-relay systems caused by terrain scattering

1. Introduction

Terrain scattering has been found to be a particularly strong mechanism for coupling interference between radio-relay systems in cases where two paths cross each other and the terrain at the intersection is visible from both the transmitting antenna of one hop and the receiving antenna of the other. In this case, the main lobes of the two antennas couple through a common area of terrain and the interference is like ground clutter received in a bi-static radar system.

In the past, interference between radio-relay systems was determined by calculations based on the mechanism of near great-circle propagation which includes line-of-sight paths, the effects of atmospheric refraction, diffraction by the surface of the Earth and tropospheric forward scatter. Such great-circle techniques combined with antenna side-lobe coupling have also been used for many years by some administrations to determine intra- and inter-system interferences in terrestrial radio-relay systems. Field measurements in recent years have indicated that great-circle propagation is often a minor contributor compared to terrain scattering.

In contrast to the case of inter-system interference, the discrepancies between great-circle predictions and measurements become smaller for intra-system interference, where the major cases have usually been between two adjacent hops on the same route.

In the case of an interference between an earth station and a terrestrial station, coupling may also occur through the main beam of the terrestrial antenna, the area around the earth station, and the side lobes of the earth station antenna. Depending on geometric circumstances, either ground scattering or great-circle coupling may be the predominant interference mechanism.

2. Mathematical model of terrain scatter

The interference power, P_r, received through the mechanism of ground scatter from a transmitting antenna radiating power, P_t, may be determined from the bi-static radar equation:

$$P_r = P_t \frac{\lambda^2}{(4\pi)^3} \int_{\Omega} \frac{G_t G_r}{R_t^2 R_r^2} \gamma \, d A_e \qquad (1)$$

where t and r denote transmitter and receiver respectively, $G(\theta,\varphi)$ is the respective antenna power gains in the direction of the scatterers in the elemental scattering area $d A_e$, θ represents the azimuth and φ the elevation from the centreline of the antenna (see Fig. 1), R_t and R_r are the respective slant distances from the antennas to the scattering element, λ is the wave length, and γ is the modified scattering coefficient describing the incoherent energy scattered by the elemental area. The elemental area $d A_e$ is defined to be the minimum of the areas of the scatterer normal to the slant vectors from the transmitter and the receiver.

Equation (1) assumes that the scattered fields from different areas or objects are incoherent, and the region Ω contains all elemental regions that contribute to the received scattered energy. In evaluating the integral for a portion of the surface of the Earth, it is necessary to account for the shadowing of individual elemental areas. Only unshadowed areas, which are visible to both the transmitting and receiving antennas, will contribute.

Comparison of measured and calculated interference values has shown that the modified scattering coefficient γ can be assumed to be constant over fairly large areas of terrain. Characteristic values of γ, which were determined by one administration for several different land covers, are given in Table 1.

FIGURE 1

Scattering from terrain

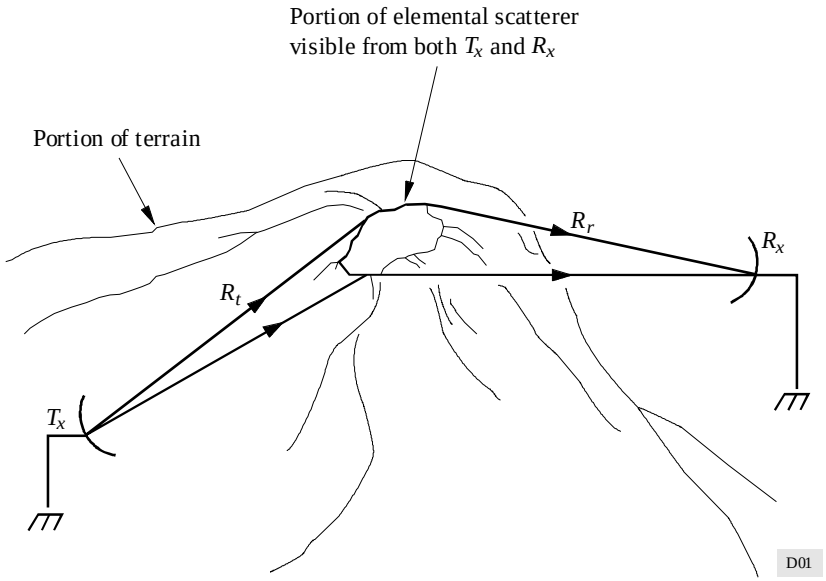

TABLE 1

Scatterer type	γ (dB)
Land cover types (from United States of America database)	
– urban residential	–8
– commercial and services	–7
– deciduous forest	–16
– mixed forest	–20
Man-made structures from FAA database	+10.4

The integral for determining the interference power, (1), may be expressed as a finite summation:

$$P_r = C_t \sum_{\Omega} \frac{G_t(p_i)\, G_r(p_i)}{R_t^2(p_i)\, R_r^2(p_i)}\, \gamma_i\, A_{e,i} \tag{2}$$

$$C_t = P_t \frac{\lambda^2}{(4\pi)^3} \tag{3}$$

where:

γ_i: coefficient of the i-th cell

p_i: cell midpoint, and

$A_{e,i}$: effective area of the i-th cell contained in the universe of cells, Ω.

Interference measurements made at a fixed frequency typically show time fluctuations around the mean value computed by equation (2). This is due to the movement of scattering objects like trees and vegetation or to temporal variations in atmospheric conditions, which may induce amplitude and phase variations between scatter returns from different scattering areas. Similarly, fluctuations about the same mean value are observed when the carrier frequency in the experiment is changed. Fortunately, for the important case of interference between digital radio systems, only the mean value given by equation (2) is of importance. On the other hand, if the strong carrier of a low-index FM signal is the source of interference then fluctuations of this carrier above the mean (upfades) have to be taken into account.

2.1 Application of the model

Practical considerations of computer resources impose a limit on the physical size of the portion of the region Ω over which the integral will be evaluated. One approach is to take the region of integration as a quadrilateral region on the surface of the Earth defined by the intersection of an azimuthal sector centred on the transmit interfering antenna with an azimuthal sector centred on the receiving interfered antenna. Figure 2 shows such a region for the case where the path from station 1 to station 4 intersects with that from station 3 to station 2, resulting in terrain scatter interference from station 1 into station 2. The sectors would be centred on the main beam azimuth of the respective antennas and could include the azimuths where the directive gain in the azimuthal direction is no more than, say, 30 dB below the maximum gain. Evaluation of the interference integral over such a region is described in § 3.1.

FIGURE 2

Interference geometry

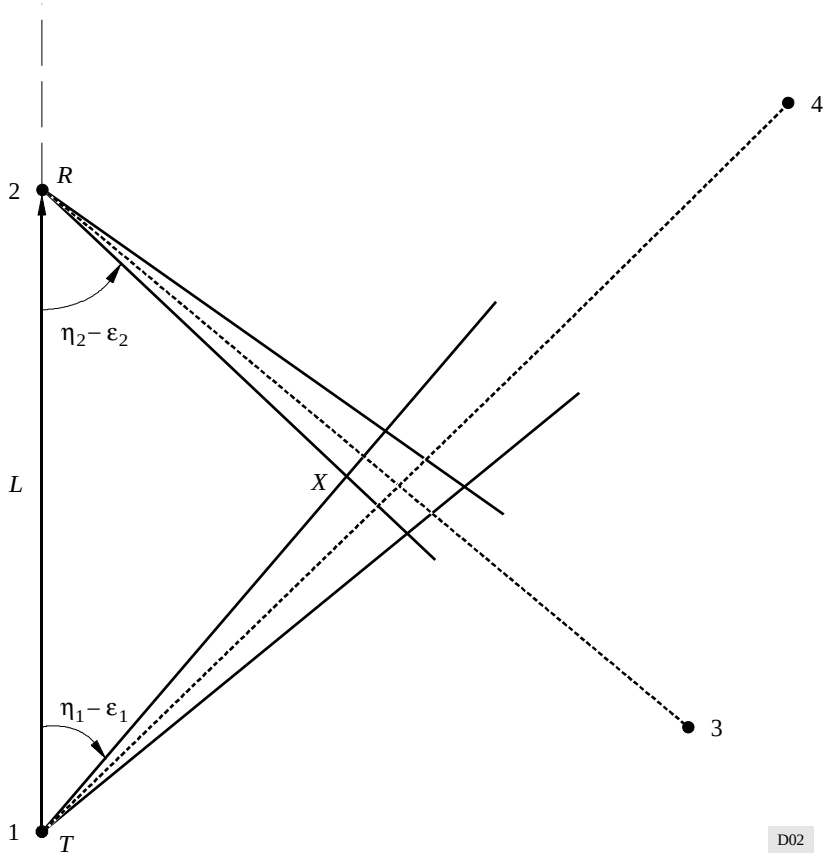

Bounding techniques offer a less arbitrary, more accurate, and more efficient means of evaluating the scatter interference power. Since most of the received energy, which has been scattered by the terrain, is usually contributed by scattering from the regions close to the intersection of the main beams of the interfering and interfered antennas, an accurate integration is only required in the vicinity of this intersection. The contribution from the remainder of Ω can be determined from an upper bound. The application of bounding techniques is described in § 3.2.

An elemental terrain area can have a non-zero contribution to the interference integral only if it is not shadowed. That is, it must be visible to both the transmitting and receiving antennas. In evaluating the shadowing of an elemental area it is necessary to consider both macro- and micro-shadowing. In macro-shadowing, an element is not visible because of obstruction by higher terrain that is closer to one of the antennas; in micro-shadowing, the element presents no effective area, $A_{e,i}$ to one of the antennas because of its orientation. The conditions necessary to determine whether an elemental region is macro- or micro-shadowed are described in § 4.1 and 4.2, respectively.

In the following developments, it is assumed that reliable digital elevation maps are available for the terrain of integration. These data take the form of elevations for a set of points defined on geodetic coordinates of latitude and longitude. While high resolution map data based on 3 arc-second intervals are available and can be used, adequate accuracy can be obtained using 15 arc-second data.

In computations, the antenna patterns are often based on measurements that are stored in computer look-up tables, or they can be analytic expressions of measured patterns. For simplicity, the readily available azimuth pattern may be rotated about the boresight axis.

3. Integration procedures

3.1 Direct evaluation

The integration over a selected region S_0 can be evaluated as:

$$P_{r,o} = C_t \sum_{p_i \in S_0} \frac{G_t(p_i)\, G_r(p_i)}{R_t^2(p_i)\, R_r^2(p_i)}\, \gamma_i\, A_{e,i} \tag{4}$$

where points p_i belong to regions $A_{e,i}$ which constitute a regular partition of the region S_0:

$$S_0 = \bigcup_i A_{e,i}, \qquad A_{e,i} \cap A_{e,j} = \varphi \qquad \text{for } i \neq j \tag{5}$$

Although the integrands are defined on a rectangular grid, it is convenient to use triads of points to define planar elemental regions. These determine triangular regions that are used to develop $A_{e,i}$ the minimal area that is visible by the transmitter and receiver:

$$A_{e,i} = min\{A_{t,i}, A_{r,i}\} \tag{6}$$

If a region is shadowed, the corresponding term is excluded from integration.

The elemental area $A_{e,i}$ is determined by the visible part of the projection of the surface ΔS_i onto the plane which is perpendicular to the ray direction (see Fig. 3):

$$A_{e,i} = min\{B_{t,i}, B_{r,i}\} \tag{7}$$

FIGURE 3
Elemental scatterer

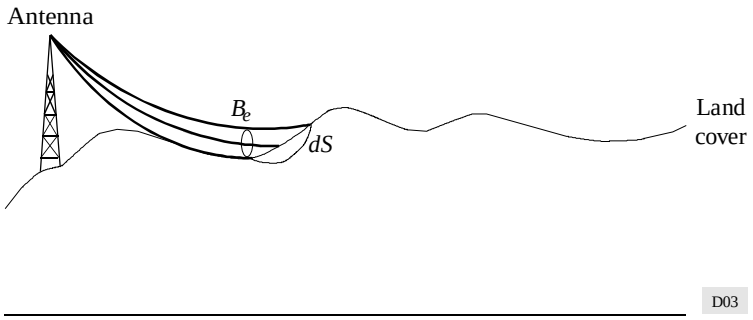

The maximal visible elemental area can be expressed as:

$$B_e = 0.5 \left[h(\sin\theta, \cos\theta) \cos(\varphi + 2\mu) + \Delta x \, \Delta y \sin(\varphi + 2\mu) \right] \tag{8}$$

$$h(u, v) = u \, \Delta z_{ba} \, \Delta y + v \, \Delta z_{bc} \, \Delta x$$

Here Δz_{ba} and Δz_{bc} are the elevation increments of the points of a grid triangle with respect to the elevation of the right angle point (see Fig. 4); Δx and Δy are the grid cell dimensions, φ and θ are the elevation and azimuth of the triangle mid-point; μ is the angle between the chord and the tangent of the scattered ray (see Fig. 5). Note that $A_{e,i}$ is the projected area onto the unit sphere of the terrain area ΔS_i which does not depend on propagation conditions.

FIGURE 4
Scatterer effective area

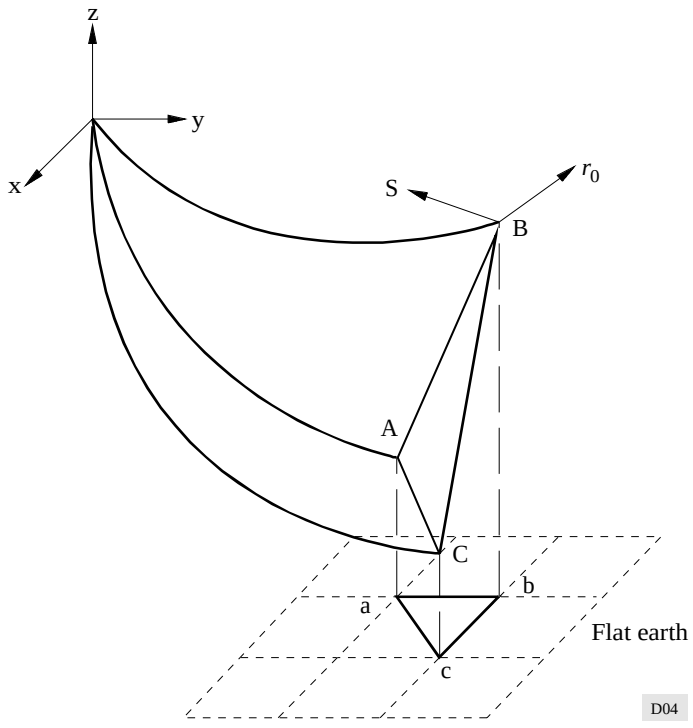

FIGURE 5

Elevation angle

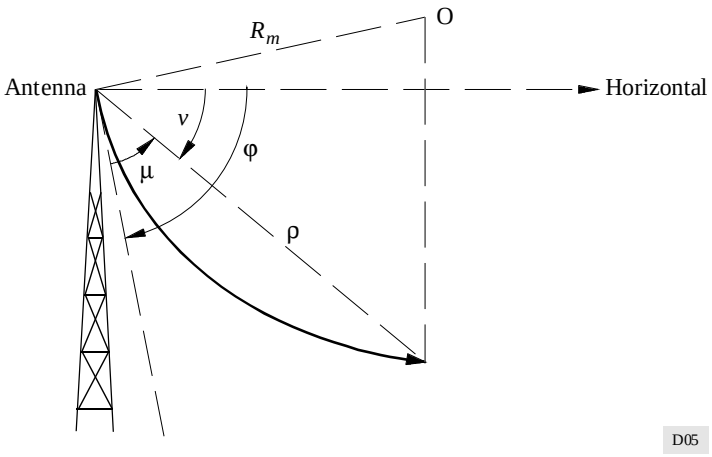

This equation does not require the calculation of any angles since it is possible to explicitly calculate all the trigonometric functions in (8):

$$\sin\theta = \frac{x}{\left(x^2 + y^2\right)^{1/2}}, \qquad \cos\theta = \frac{y}{\left(x^2 + y^2\right)^{1/2}}$$

$$\sin(\varphi + 2\mu) = \frac{z}{\rho}\left(1 - \frac{\rho^2}{4R_e^2}\right)^{1/2} + \frac{d}{2R_e} \tag{9}$$

$$\cos(\varphi + 2\mu) = \frac{d}{\rho}\left(1 - \frac{\rho^2}{4R_e^2}\right)^{1/2} - \frac{z}{2R_e}$$

where $\rho = (x^2 + y^2 + z^2)^{1/2}$ is the distance between the antenna and scatterer, $d = (x^2 + y^2)^{1/2}$ is its projection onto the horizontal plane, $R_e = a \cdot k$, a is the radius of the Earth, k is the Earth radius factor that depends on the refractivity gradient in the atmosphere.

The substitution of (9) into (8) gives:

$$B_e = 0.5\left[h(x, y)\left(\frac{1}{\rho} - \frac{z}{2dR_e}\right) + \Delta x\,\Delta y\left(\frac{z}{\rho} + \frac{d}{2R_e}\right)\right] \tag{10}$$

where (x, y, z) are the coordinates of the triangle mid-point. Since $z << R_e$, the above equation can be simplified:

$$B_e = \frac{0.5}{\rho}\left[h(x, y) + \Delta x\,\Delta yz\right] + \frac{d}{4R_e}\Delta x\,\Delta y \tag{11}$$

3.2 Bounding techniques

A recursive technique for computing P_r may be developed by partitioning the universe Ω into two mutually exclusive subsets S_0 and Q_0:

$$S_0 \cup Q_0 = \Omega, \qquad S_0 \cap Q_0 = \varphi \tag{12}$$

and representing the integral (1) as a sum of two integrals:

$$P_r = C_t \int_{S_0} \frac{G_t\,G_r}{R_t^2\,R_r^2}\,\gamma\,d\,A_e + C_t \int_{Q_0} \frac{G_t\,G_r}{R_t^2\,R_r^2}\,\gamma\,d\,A_e \tag{13}$$

This expression is evaluated by numerically integrating the first term and bounding the second. If the bound is much less than the computed value of the first integral, then the integral over the universe Ω can be replaced by the integral over S_0. The needed accuracy of estimation determines how small the bound must be compared to the integral. In most applications, if the bound is less than 0.1 times the integral, the integral over the universe Ω can be replaced by the integral over S_0, leading to an error of less than 0.41 dB in the estimation of P_r. It is reasonable to accept such an error in estimation especially given the uncertainties in determining scatter coefficients and map coordinates. In general, since antennas are highly directive, the region S_0 of exact integration is significantly smaller than the whole region.

If the bound over Q_0 is not much less than the integral over S_0, replace the region of integration S_0 with a larger region $S_0 \cup S_1$ ($S_1 \subset Q_0$). Define Q_1 as the complement of S_1 with respect to Q_0 so that $S_1 \cup Q_1 = Q_0$ and $S_1 \cap Q_1 = \varphi$. Evaluate the bound over Q_1. Since the integral over Q_1 cannot be greater than the integral over Q_0, the bound over Q_1 is, in general, less than the bound over Q_0. Also the integral over $S_0 \cup S_1$ must be larger than the integral over S_0. Hence, if the process is repeated n times, the bound becomes less than the integral over $\cup_i S_i$, allowing the integral over the universe Ω to be replaced by the integral over the subset $\cup_i S_i$. In practice, it is desirable for n to be small, say one or two. This can be achieved by properly choosing S_0 and devising the algorithm so that the bound over Q_0 (and other Q_i) is as tight as possible.

Note that it is possible to add S_is to the actual integration area and make use of earlier results so that integration over any area S_i is carried out only once. Since the bounds are easier to compute, this process may be repeated as often as needed for the accuracy of estimation.

The evaluation of the upper bounds, Q_0, Q_1, ..., makes use of the inequality $\gamma\, d\, A_e \le \gamma\, R_t^2\, d\omega_t$, where $d\omega_t$ is the solid angle with the centre at the antenna of the element dS (see Note). Using spherical coordinates with the centre at the transmitter,

$$P_{r,e} = C_t \int_{Q_0} \frac{G_t\, G_r}{R_r^2\, R_t^2}\, \gamma\, d\, A_e \le C_t \max_{Q_0} \left[\frac{\gamma G_t\, G_r}{R_r^2}\right] D_0 \tag{14}$$

where D_0 is the area of the projection of the integration region Q_0 onto the unit sphere with the centre at the transmitter, and φ_t and θ_t are the elevation and azimuth of the elemental scatterer.

Since:

$$\max_{Q_0} \left[\frac{\gamma G_t\, G_r}{R_r^2}\right] \le \frac{\gamma_{max}\, G_{t,max}\, G_{r,max}}{R_{r,min}^2} \tag{15}$$

where maxima and minimum are taken over the region Q_0:

$$P_{r,e} \le C_t\, \frac{G_{t,max}\, G_{r,max}}{R_{r,min}^2}\, \gamma_{max}\, D_0 \tag{16}$$

Using spherical coordinates with the centre at the receiver, gives the analogous result:

$$P_{r,e} \le C_t\, \frac{G_{t,max}\, G_{r,max}}{R_{t,min}^2}\, \gamma_{max}\, D_0 \tag{17}$$

The tighter of these two bounds has the form:

$$P_{r,e} \le C_t \frac{G_{t,max}\, G_{r,max}}{R_m^2}\, \gamma_{max}\, D_0 \tag{18}$$

where:

$$R_m = max\, \{R_{r,min}, R_{t,min}\} \tag{19}$$

Different bounds can be found by selecting different regions S_0. In the most important case S_0 represents a terrain region that lies on the intersection of the angles $| \theta_{r,0} - \theta_r | < \varepsilon_1$, $| \theta_{t,0} - \theta_t | < \varepsilon_2$, where $\theta_{r,0}$ and $\theta_{t,0}$ are the antenna direction azimuths (see Fig. 2). If ε_1 and ε_2 are such that antenna gains inside the angles are greater than local maxima at their side lobes, then the above bound can be rewritten as:

$$P_{r,e} \leq C_t \frac{G_r(\theta_{r,0} + \varepsilon_1, \varepsilon_1)\, G_t(\theta_{t,0} + \varepsilon_2, \varepsilon_2)}{R_m^2} \gamma_{max} D_0 \tag{20}$$

In this particular case, $R_{t,min}$ and $R_{r,min}$ can be found from the triangle RXT shown in Fig. 2.

$$R_{t,min} = \frac{L \sin(\eta_2 - \varepsilon_2)}{\sin(\eta_1 + \eta_2 - \varepsilon_1 - \varepsilon_2)} \tag{21}$$

$$R_{r,min} = \frac{L \sin(\eta_1 - \varepsilon_1)}{\sin(\eta_1 + \eta_2 - \varepsilon_1 - \varepsilon_2)}$$

The method of calculating the area D_0 is presented in Annex 2. However, to avoid complex calculations, this area can be bounded by the total area of the unit sphere which is equal to 4π.

The preceding bounds were based on antenna directivity. Other bounds may be developed from equation (2). For instance, remote regions can be excluded from the integration. The corresponding bound has the following form:

$$P_{r,x} \leq C_t \frac{G_r(\theta_{r,0}, 0)\, G_t(\theta_{t,0}, 0)}{R^2} \gamma_{max} \bar{D}_0 \tag{22}$$

where $\bar{D}_0$ is the area of the projection of the region S_0 onto the unit sphere, R is selected such that $P_{r,x} + P_{r,e}$ is smaller than the required accuracy.

Note from the Director, BR – For information, the derivation of this evaluation is given in:

SMITH, W.E., SULLIVAN, P.L., GIGER, A.J. and ALLEY. G.D. [June, 1987] Recent advances in microwave interference prediction. IEEE International Conference on Communications (ICC ’87), paper 23.2.

4. Shadowing

4.1 Macro-shadowing

Since the shadowing of an elemental area can be related to the shadowing of its individual points, it is necessary to determine the shadowing of constituent points. It would be convenient to use spherical coordinates with the centre at the antenna for this purpose. In shadowing calculations using a spherical coordinate system, an algorithm has only to keep track of the largest launch angle along the radial plane, updating the maximum launch angle only as needed.

The shadowing concepts do not change when a grid coordinate system is used, but the determination of visibility of any grid point cannot easily be carried out, since there is no guarantee that one or more grid points can be found with the same azimuth as the test point. An approximation of the maximum launch angle along the radial must be made so that the launch angle of the test point can be compared to this value to determine its visibility. For a given test point P, one must first determine the two grid points Q and R which are closer than the test point, straddle the radial from the antenna to the test point, have minimum azimuth difference, and have minimal launch angles. The projection of these points onto the horizontal plane is shown in Fig. 6.

FIGURE 6

Shadowing of the test point P using visible launch angles at points Q and R

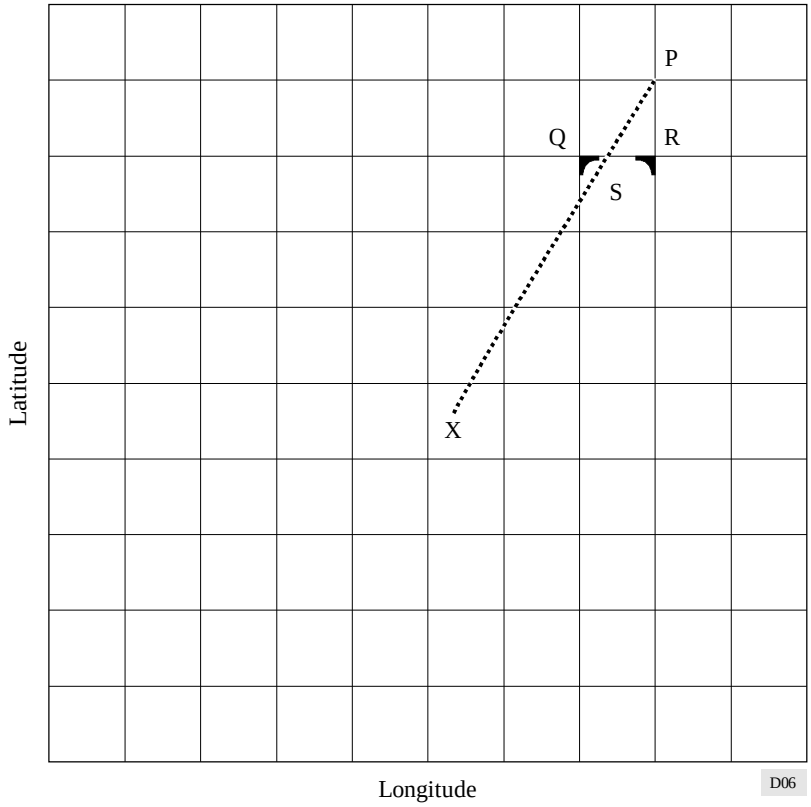

It is necessary to compare the launch angle to the test point P with the visible launch angle that can be associated with the point of intersection S of the radial plane with the line segment joining the two grid points. This radial plane is shown in Fig. 7. One compares the launch angle φ_S to φ_P and decides that point P is visible if and only if $\varphi_P \geq \varphi_S$, assuming S is visible. Otherwise, it is shadowed, or not visible.

The launch angle φ of any point can be derived from Fig. 5:

$$\varphi = \arcsin\left[\frac{z}{\rho}\left(1 - \frac{\rho^2}{4R_e^2}\right)^{1/2} - \frac{d}{2R_e}\right] \tag{23}$$

where:

$R_e = k \cdot a$

k: effective Earth radius factor, which depends on the refractivity gradient

a: Earth radius

d: horizontal distance between the antenna and the test point

z: elevation of the test point over the antenna

$\rho = (x^2 + y^2 + z^2)^{1/2}$.

Since arc sin(x) is a monotonically increasing function, it is only necessary to compare the arguments of the arc sin function in determining the visibility of P given that S is visible. Since $\rho << R_e$, the criterion for the point P to be shadowed by the point S can be written as

$$\frac{z_p}{\rho_p} - \frac{d_p}{2R_e} < \frac{z_s}{\rho_s} - \frac{d_s}{2R_e} \tag{24}$$

In the case of a grid coordinate system, the launch angle φ_S at point S may be determined by linear interpolation:

FIGURE 7

Shadowing of the test point P

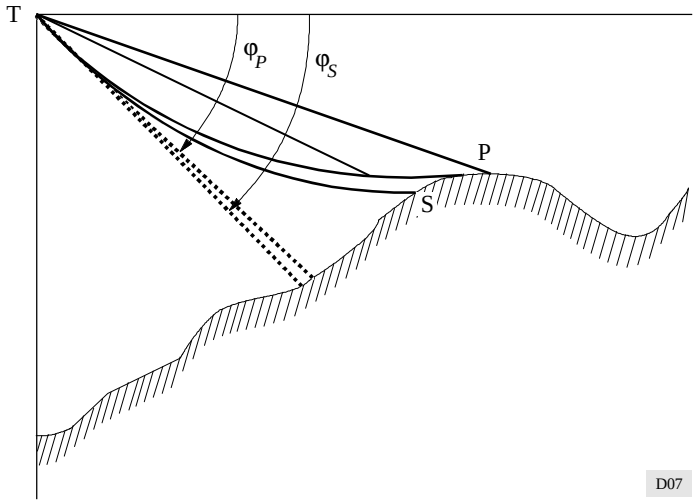

$$\varphi_S = \frac{d_{QS}}{d_{QR}}\ \varphi_Q + \frac{d_{RS}}{d_{QR}}\ \varphi_R \tag{25}$$

where:

d_{QS}: distance between Q and S

d_{QR}: distance between Q and R

d_{RS}: distance between R and S.

In shadowing, one starts with the grid points closest to the transmitter and assumes that they are visible. One moves out from these points in concentric rectangles so that the whole grid is covered and shadowing of all points is determined.

4.2 Micro-shadowing

The micro-shadowing of an elemental area is determined by its orientation. Consider the elemental triangular area in Fig. 4. This triangle is micro-shadowed if and only if its surface outer normal N and the unit tangent vector r_0 of the corresponding ray are acute. This can be written as

$$N \cdot r_0 \geq 0 \tag{26}$$

Let z_a, z_b and z_c be the elevations at the three adjacent points on the grid (see Fig. 4) and at least one of these points is not shadowed. The vertices of the triangle ABC that approximates the surface element can be defined by their Cartesian coordinates: $A(x_b, y_b + \Delta y, z_a)$, $B(x_b, y_b, z_b)$, $C(x_b + \Delta x, y_b, z_c)$. Assume that $\angle abc = 90°$. Then inequality (26) is equivalent to (see Note):

$$\delta\left[h(\sin\theta, \cos\theta)\cos(\varphi + 2\mu) + \Delta x\,\Delta y \sin(\varphi + 2\mu)\right] \geq 0$$

$$h(u, v) = u\,\Delta z_{ba}\,\Delta y + v\,\Delta z_{bc}\,\Delta x \tag{27}$$

$$\delta = \text{sign}\,(\Delta x\,\Delta y)$$

where φ is the launch angle, μ is the difference between the launch angle and the elevation angle, and θ is the azimuth of the scatterer. One half of the absolute value of the left-hand side of this inequality is equal to the scatterer effective area as given by equation (8). Therefore, in calculating an elemental scatter interference, one can evaluate the left-hand side of expression (27) and use it also for micro-shadowing.

A simplified approximate method of determining micro-shadowing and evaluating B_e, the effective area of an elemental triangle, is given in Annex 3. This method reduces the calculation time by using a first order approximation in φ to equations (11) and (27). It may be used whenever the launch angles to the region near the intersection of the main beams of the interfering and interfered antennas are less than about 5°, in which case the errors introduced are less than 10%.

Note from the Director, BR – For information, the derivation of this equation is given in:

KAHN, A.L., PRABHU, V.K. and TURIN, W. [1991] Shadowing algorithms in estimating ground scatter interference. Conf. Record, IEEE Global Telecommunications Conference (GLOBECOM '91).

ANNEX 2

Calculation of the area of a quadrilateral on the unit sphere

The area of the quadrilateral, D_0 is given by the formula

$$D_0 = A_1 + A_2 + A_3 + A_4 - 2\pi \tag{28}$$

where A_1, A_2, A_3 and A_4 are the angles of the quadrilateral on the unit sphere.

The angle A_i is equal to the angle between the planes containing the centre of the sphere and the great circles that form this angle. The angle can be obtained from the equation

$$\cos A_i = \frac{\mathrm{N_j} \cdot \mathrm{N_k}}{N_j \cdot N_k} \tag{29}$$

where $\mathrm{N_j}$ and $\mathrm{N_k}$ are the normals of the planes, N_j and N_k are their lengths. These vectors are given by the cross-products of the radius-vectors of the corresponding points on the surface of the sphere. For example, denoting the radius-vector of the vertex A_i as r_i,

$$\cos A_2 = \frac{(r_2 \times r_1) \cdot (r_3 \times r_2)}{|r_2 \times r_1| \cdot |r_3 \times r_2|} \tag{30}$$

To derive explicit equations consider Cartesian and spherical coordinates with the origin at the centre of the sphere, then the radius-vector of the point A_i on the unit sphere can be expressed as:

$$r_i = \{\cos \varphi_i \sin \theta_i, \cos \varphi_i \cos \theta_i, \sin \varphi_i\} \tag{31}$$

The cross-product of these vectors is equal to:

$$r_{ij} = r_i \times r_j = \{x_{ij}, y_{ij}, z_{ij}\} \tag{32}$$

where:

$$\begin{aligned} x_{ij} &= \cos \varphi_i \cos \theta_i \sin \varphi_j - \cos \varphi_j \cos \theta_j \sin \varphi_i \\ y_{ij} &= \cos \varphi_j \sin \theta_j \sin \varphi_i - \cos \varphi_i \cos \theta_i \sin \varphi_j \\ z_{ij} &= \cos \varphi_i \sin \theta_i \cos \varphi_j \cos \theta_j - \cos \varphi_j \sin \theta_j \cos \varphi_i \cos \theta_i \end{aligned} \tag{33}$$

The inner product of cross-products in equation (30) is given by

$$r_{ij} \cdot r_{kl} = x_{ij} x_{kl} + y_{ij} y_{kl} + z_{ij} z_{kl} \tag{34}$$

and the vector length:

$$r_{ij} = \left(x_{ij}^2 + y_{ij}^2 + z_{ij}^2 \right)^{1/2} \tag{35}$$

ANNEX 3

Alternative method of calculating effective area and micro-shadowing

For small launch angles and azimuth variations within a triangular region such as shown in Fig. 4, micro-shadowing may be determined approximately by first sorting the triangle vertices by azimuth: $P_1(\rho_1, \varphi_1, \theta_1)$, $P_2(\rho_2, \varphi_2, \theta_2)$, $P_3(\rho_3, \varphi_3, \theta_3)$

$$\theta_1 \le \theta_2 \le \theta_3 \tag{36}$$

Using linear interpolation determine the coordinates of the point P_x that lies at azimuth θ_2 on the line connecting P_1 and P_3. If point P_2 lies farther from the antenna than P_x and its elevation is less than that of P_x, the area is micro-shadowed. Similarly, the area is micro-shadowed if point P_2 lies closer to the antenna than P_x and its elevation is higher than that of P_x.

Define the elevation of point P_2 minus that of point P_x as $\Delta\varphi$ and the amount by which the distance of point P_2 from the antenna exceeds that of point P_x as $\Delta\rho$. A cell is micro-shadowed if:

$$\Delta\rho \cdot \Delta\varphi \le 0 \tag{37}$$

where:

$$\begin{aligned} \Delta\rho &= \rho_2 - \rho_1 \frac{\theta_3 - \theta_2}{\theta_3 - \theta_1} - \rho_3 \frac{\theta_2 - \theta_1}{\theta_3 - \theta_1} \\ \Delta\varphi &= \varphi_2 - \varphi_1 \frac{\theta_3 - \theta_2}{\theta_3 - \theta_1} - \varphi_3 \frac{\theta_2 - \theta_1}{\theta_3 - \theta_1} \end{aligned} \tag{38}$$

The effective projected area of the triangle may be approximated by:

$$B_e = \frac{\rho^2 \cos \varphi}{2} |\Delta A| \tag{39}$$

where ρ is the distance from the antenna to the elemental triangle, and:

$$\Delta A = (\theta_3 - \theta_1) \Delta\varphi \tag{40}$$

Thus, the value Δφ can be used not only for micro-shadowing, but also for estimating the projected area. Note that since θ is measured modulo 2π and the elemental triangles have a small extent in azimuth, any difference $\theta_i - \theta_j$ in equations (38) and (40) must be reduced by 2π if it exceeds π.